

A New Synthesis of Mesoporous MSU-X Silica Controlled by a Two-Step Pathway

Cédric Boissière,[†] André Larbot,[†] Arie van der Lee,[†] Patricia J. Kooyman,[‡] and Eric Prouzet^{*,†}

Laboratoire des Matériaux et Procédés Membranaires (CNRS UMR 5635), E.N.S.C.M., 8 rue de l'École Normale, F-34296 Montpellier Cedex 5, France, and National Centre for HREM, Delft University of Technology, Rotterdamseweg 137, 2628 AL Delft, The Netherlands

Received December 8, 1999. Revised Manuscript Received June 15, 2000

In the field of micelle templated structures (MTS), the MSU-X family of mesoporous silica is obtained by using nonionic poly(ethylene oxide)-based surfactants. We show that the microstructure of these materials is highly dependent on the initial pH conditions and that a first assembly step, using a mild acidity, which allowed us to obtain a stable solution containing micellar hybrid objects made of both surfactant micelles and small silica oligomers, can be determined in the 2–4 pH range. The second step of the synthesis consists of the condensation of the silica particles and can be performed in two different ways. Either the pH of the stable solution is increased to neutral values or small amounts of fluoride are added. With the second method both the nanostructure and the particle morphology are better controlled. This novel two-step synthesis leads in addition to hexagonal pore framework when assembly molecules such as Tween 60 or block copolymer Pluronic P123 are used as assembly agents.

1. Introduction

The rediscovery^{1,2} of highly porous micelle templated structures (MTS)^{3,4} by a research group of Mobil Co. and shortly thereafter by Inagaki et al.^{5,6} has attracted considerable attention due to the fact that these materials offer a large surface area ($\sim 1000 \text{ m}^2 \text{ g}^{-1}$) and porous volume ($\sim 1 \text{ cm}^3 \text{ g}^{-1}$) with a mesoporous narrow pore size distribution that can be adjusted between 2 and 10 nm. Since, the field of research of these materials called MCM-41 and -48 for the hexagonal and the cubic structure, respectively (MCM for Mobil Crystalline Material), obtained through an assembly mechanism between organic surfactants (originally long chain quaternary ammonium compounds) and inorganic species, has been greatly enlarged to new inorganic frameworks (i.e. non alumino-silicate).⁷ Other surfactants, such as anionic,⁸ neutral,⁹ and poly(ethylene oxide) (PEO) non-

ionic¹⁰ ones, also led to different mesoporous silicas. The latter gave materials reported as MSU-V,¹¹ MSU-G,¹² or MSU-X (X = 1 to 4) (MSU for Michigan State University) where X refers to the surfactant molecules that can be either alkyl-PEO, alkyl-aryl PEO, polypropylene oxide PEO block-copolymers, or ethoxylated derivatives of the fatty esters of sorbitan (Tween), respectively.^{10,13} In the range of PEO-based nonionic surfactant two families could be identified: the MSU-X compounds usually prepared in neutral pH,^{10,14} and the SBA compounds (SBA for Santa Barbara) mainly using block copolymers with a pH equal to or lower than one.^{15,16} A third synthesis pathway that did not use a real assembly mechanism but a confined aqueous structure defined in the lyotropic liquid crystal domain, was also very successful to provide both very well organized materials and thin films through an elegant process.^{17–19}

Unlike materials of the SBA family (e.g., SBA-15) that exhibit either hexagonal or cubic symmetries,^{15,16} MSU-X

* To whom correspondence should be addressed. E-mail: prouzet@cit.enscm.fr.

[†] Laboratoire des Matériaux et Procédés Membranaires.

[‡] Delft University of Technology.

(1) Kresge, C. T.; Leonowicz, M. E.; Roth, W. J.; Vartuli, J. C.; Beck, J. S. *Nature* **1992**, *359*, 710.

(2) Beck, J. S.; Vartuli, J. C.; Roth, W. J.; Leonowicz, M. E.; Kresge, C. T.; Schmitt, K. D.; Chu, C. T.-W.; Olson, D. H.; Sheppard, E. W.; McCullen, S. B., et al. *J. Am. Chem. Soc.* **1992**, *114*, 10834.

(3) Chiola, V.; Ritsko, J. E.; Vanderpool, C. D. US Patent 3 556 725 1971.

(4) Di Renzo, F.; Cambon, H.; Dutartre, R. *Microporous Mater.* **1997**, *10*, 283.

(5) Inagaki, S.; Fukushima, Y.; Kuroda, K. *J. Chem. Soc., Chem. Commun.* **1993**, 680.

(6) Inagaki, S.; Fukushima, Y.; Kuroda, K. In *Zeolites and Related Microporous Materials: State of the Art*; Weitkamp, J., Karge, H. G., Pfeifer, H., Hölderich, W., Ed.; Elsevier Science: New York, 1994; Vol. 84, pp 125.

(7) Beck, J. S.; Vartuli, J. C. *Curr. Opin. Solid State Mater. Sci.* **1996**, *1*, 76.

(8) Huo, Q.; Margolese, D. I.; Ciesla, U.; Demuth, D. G.; Feng, P.; Gier, T. E.; Sieger, P.; Firouzi, A.; Chmelka, B. F.; Schüth, F., et al. *Chem. Mater.* **1994**, *6*, 1176.

(9) Tanev, P.; T.; Pinnavaia, T. J. *Science* **1995**, *267*, 865.

(10) Bagshaw, S. A.; Prouzet, E.; Pinnavaia, T. J. *Science* **1995**, *269*, 1242.

(11) Tanev, P.; T.; Pinnavaia, T. J. *Science* **1996**, *271*, 1267.

(12) Kim, S.-S.; Zhang, W.; Pinnavaia, T. J. *Science* **1998**, *282*, 1302.

(13) Prouzet, E.; Cot, F.; Nabias, G.; Larbot, A.; Kooyman, P. J.; Pinnavaia, T. J. *Chem. Mater.* **1999**, *11*, 1498.

(14) Prouzet, E.; Pinnavaia, T. J. *Angew. Chem., Int. Ed. Engl.* **1997**, *36*, 516.

(15) Zhao, D.; Feng, J.; Huo, Q.; Melosh, N.; Fredrickson, G. H.; Chmelka, B. F.; Stucky, G. D. *Science* **1998**, *279*, 548.

(16) Zhao, D.; Huo, Q.; Feng, J.; Chmelka, B. F.; Stucky, G. D. *J. Am. Chem. Soc.* **1998**, *120*, 6024.

(17) Attard, G. S.; Glyde, J. C.; Göltner, C. G. *Nature* **1995**, *378*, 366.

materials generally possess a 3D worm-hole porous framework with poorly defined crystallographic symmetry, which is expected to enhance the diffusion rate of reacting species and does not require any specific orientation for the design of filtration layers. Nevertheless, it was shown recently that a postsynthesis hydrothermal treatment could result in a hexagonal structure that was labeled SAB (SAB for Steven A. Bagshaw).²⁰ Compared with syntheses using quaternary ammonium compounds and inorganic precursors instead of alkoxides, the higher cost of the MSU-X synthesis implied by using tetraethyl orthosilicate (TEOS: $\text{Si}(\text{O}(\text{CH}_2\text{CH}_3)_4)$) as the silica source is balanced by the lower cost of nonionic surfactants and the synthesis at atmospheric pressure that does not request specific autoclaves as M41S materials do. For instance, if alkoxides can hardly be used as silica sources for the preparation of large amounts of catalysts, their higher cost should not be a drawback for specific applications such as high-pressure liquid chromatographic columns or supported filtration layers. In addition, Sierra and Guth recently published a new strategy involving a nonionic surfactant (Triton $\times 100$) and sodium silicate, which could be a successful approach for the further synthesis of large batches of low-cost mesoporous materials.²¹

One purpose of these syntheses is to be able to tailor by slight changes the material pore size. This is usually achieved by changing the surfactant, that is the hydrophobic chain length, or by adding swelling agents such as trimethyl-1,3,5-benzene (TMB).² Postsynthesis treatments can be successful too,^{22–24} and it has been shown also that both pore size and wall thickness can be adjusted by varying the synthesis temperature when nonionic surfactants are used as assembling agents.^{14,15} Compared with MCM-41 materials for which a strict pH adjustment is required to obtain materials with good crystallinity,^{25,26} syntheses of MSU-X are less drastically bound to this condition when neutral conditions are allowed by the use of fluoride ions as hydrolysis catalysts of the silicon precursor (fluoride is removed upon further calcination).¹⁴ Unlike the syntheses of SBA materials that require a highly acidic medium between protonated species, the MSU-X assembly mechanism is based on weak interactions between the PEO chains and neutral species. Therefore, the synthesis of MSU-X, which occurs at neutral pH can thus be further adjusted to tailor the weak interactions between TEOS molecules and PEO chains in order to modify the final structure. The addition of salts has been shown to modify the structure of these systems, too.^{27,28} However, the more

the synthesis is dependent on various parameters, the more work has to be done to bring a better reproducibility coupled with a high yield as well as an accurate control and understanding of the synthesis mechanism.

We recently reported that a correct pH adjustment of the solution of surfactant and TEOS could lead to a colorless micellar solution that remained stable for several days.²⁹ This allowed us to define a double-step synthesis (the assembly and condensation steps being separated) that can be shortly described as follows. First, after an initial mixing of TEOS and surfactant leading to a milky emulsion, an assembly step is obtained by the pH adjustment around pH 2 of this solution, which gave a homogeneous and colorless solution containing 6 to 7 nm monodisperse micellar hybrid objects, as proved by light scattering results. This solution is stable for days. This assembly step is followed by the silica condensation step allowed by the addition of fluoride. In that case, the condensation step occurred only when fluoride was added and it happened only in a homogeneous medium at the nanometric scale, where a classical nucleation–growth process is observed. Monodisperse particles suitable for HPLC chromatography could be obtained through this process and we showed recently that less expensive silica precursors such as sodium silicate or colloidal silica could be used.^{29–31} This present paper reports the full achievement of the study of the pH influence on the final structure of MSU-X. We describe how changing the pH of the initial surfactant solution can drastically modify both the morphology and the nanostructure of the final material. This first study helped us to discover better conditions for the new double-step synthesis pathway that was briefly described previously.²⁹ This new pathway can be applied to a wide family of nonionic surfactants or copolymers and different synthesis parameters can be adjusted to control the final structure. It is illustrated by different examples, one leading to micrometric spherical particles, the other to a hexagonal MCM-41-like material, which shows how versatile the nonionic synthesis pathway is.

2. Experimental and Synthesis

2.1. Experimental. Various PEO surfactants with different molecular structures were used to form the MSU-X silicates. These structures were synthesized with Triton X-100 (Grosseron Chemicals), Tergitol 15-S-N ($\text{CH}_3(\text{CH}_2)_{14}(\text{EO})_N\text{OH}$), kindly provided by Union Carbide Co., Tween 20 (PEO sorbitan monolaurate) (Fluka Chemicals), Tween 40 (PEO sorbitan monopalmitate) (Sigma Chemicals), Tween 60 (PEO sorbitan monostearate) (Sigma Chemicals), triblock copolymer ($\text{EO}_{20}\text{PO}_{70}\text{EO}_{20}$) Pluronic P 123 (BASF), tetraethoxysilane TEOS (Acros chemicals), and sodium fluoride (Fluka Chemicals). All reagents were used as received. The materials were characterized by Scanning Electron Microscopy (SEM), X-ray diffraction, nitrogen adsorption and Transmission Electron Microscopy (TEM). TEM was performed using a Philips CM30 T electron microscope with a LaB₆ filament as a source of

(18) Attard, G. S.; Coleman, N. R. B.; Elliott, J. M. In *Mesoporous Molecular Sieves 1998*; Bonnevot, L., Beland, F., Danumah, C., Giasson, S., Kaliaguine, S., Eds.; Elsevier Science: Amsterdam, 1998; Vol. 117, p 89.

(19) Attard, G. S.; Bartlett, P. N.; Coleman, N. R. B.; Elliott, J. M.; Owen, J. R.; Wang, J. H. *Science* **1997**, *278*, 838.

(20) Bagshaw, S. A. *J. Chem. Soc., Chem. Commun.* **1999**, 271.

(21) Sierra, L.; Guth, J. L. *Microporous Mesoporous Mater.* **1999**, *27*, 243.

(22) Khushalani, D.; Kuperman, A.; Ozin, G. A.; Tanaka, K.; Garcès, J.; Olken, M. M.; Coombs, N. *Adv. Mater.* **1995**, *7*, 842.

(23) Huo, Q.; Margolese, D. I.; Stucky, G. D. *Chem. Mater.* **1996**, *8*, 1147.

(24) Bagshaw, S. A. In *Mesoporous Molecular Sieves 1998*; Bonnevot, L., Beland, F., Danumah, C., Giasson, S., Kaliaguine, S., Eds.; Elsevier Science: Amsterdam, 1998; Vol. 117, p 381.

(25) Coustel, N.; Di Renzo, F.; Fajula, F. *J. Chem. Soc., Chem. Commun.* **1994**, 967.

(26) Ryoo, R.; Kim, J. M. *J. Chem. Soc., Chem. Commun.* **1995**, 711.

(27) Zhang, W.; Glomski, B.; Pauly, T. R.; Pinnavaia, T. J. *J. Chem. Soc., Chem. Commun.* **1999**, 1803.

(28) Bagshaw, S. A. *J. Chem. Soc., Chem. Commun.* **1999**, 1785.

(29) Boissière, C.; van der Lee, A.; El Mansouri, A.; Larbot, A.; Prouzet, E. *J. Chem. Soc., Chem. Commun.* **1999**, 20, 2047.

(30) Boissière, C.; Larbot, A.; Prouzet, E. in *Nanoporous Materials II*; Sayari, A., Jaroniec, M., Pinnavaia, T. J., Eds.; Elsevier Science BV.: Banff, Alberta, Canada, 2000; Vol. 129, p 31.

(31) Boissière, C.; Larbot, A.; Prouzet, E. *Chem. Mater.*, in press.

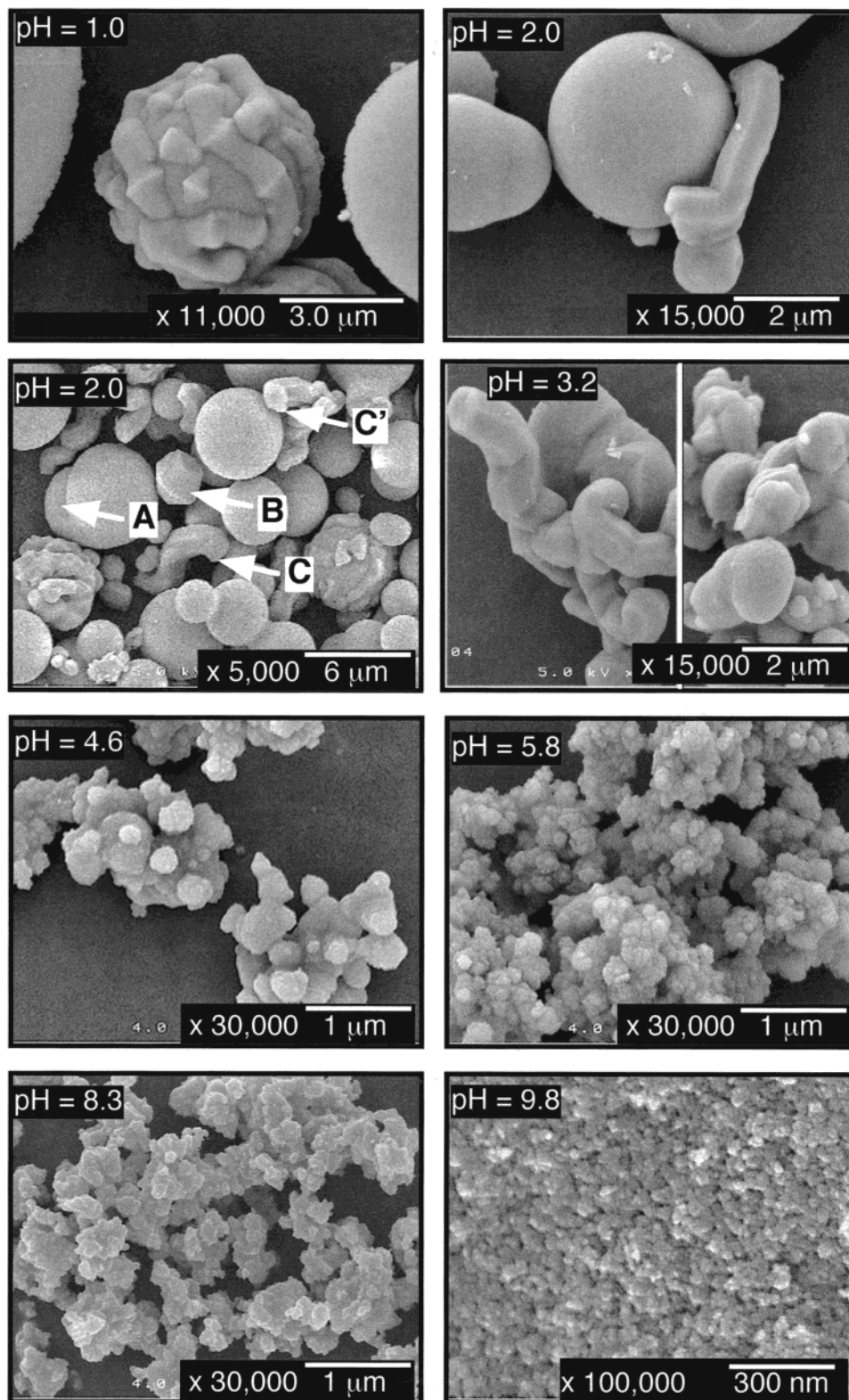


Figure 1. SEM observations of calcined MSU-2 silica synthesized with aqueous solutions of Triton X 100 preliminarily adjusted at different pHs. As the pH increases from 1.0 to 9.8, the mean size of particles decreases from well-defined micrometric size particles to ill-defined nanometric ones.

electrons operated at 300 kV. Samples were mounted on a microgrid carbon polymer supported on a copper grid by placing a few droplets of a suspension of ground sample in ethanol on the grid, followed by drying at ambient conditions. SEM micrographs were obtained on a Hitachi S-5400 FEG microscope. Nitrogen adsorption isotherms were measured at 77 K on a Micromeritics 2010 Sorptometer using standard continuous procedures, and samples first degassed at 150 °C

for 15 h. Surface areas were determined by the BET method in the 0.05–0.2 relative pressure range^{32,33} and pore size distribution by a polynomial relationship based on the Broekhoff

(32) Brunauer, S.; Emmet, P. H.; Teller, E. *J. Am. Chem. Soc.* **1938**, *60*, 309.

(33) Brunauer, S.; Deming, L. S.; Deming, W. S.; Teller, E. *J. Am. Chem. Soc.* **1940**, *62*, 1723.

Table 1. Physicochemical Properties of Calcined MSU-2 Silica Synthesized with Triton X 100 at Different Initial pH

pH	d spacing (nm)	fwhm ^a (nm)	pore size ^b (nm)	wall thickness ^c (nm)	surface area (m ² g ⁻¹)	V_p^d (cm ³ g ⁻¹)
0.0	3.7	1.3	≤2.5	≥1.2	700	0.34
1.0	3.7	1.6	≤2.5	≥1.2	692	0.33
2.0	3.7	1.4	≤2.5	≥1.2	980	0.47
3.1	4.4	2.9	2.7	1.7	695	0.48
4.6	4.7	2.6	3.1	1.6	750	0.60
5.8	5.0	2.3	3.7	1.3	655	0.70
6.1	5.1	2.7	3.7	1.4	630	0.67
8.3	5.2	3.1	3.7	1.5	580	0.82
9.8			<2.0 to <20.0		450	1.0

^a Full width at half maximum. ^b BdB desorption average pore diameter. ^c Due to the disordered porous framework, wall thickness was calculated by subtracting the pore diameter from the d spacing. ^d V_p was determined as the total adsorbed volume for $P/P_0 \approx 0.99$.

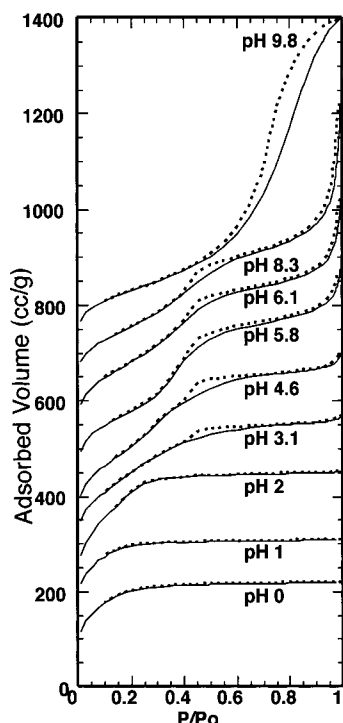


Figure 2. Evolution of the nitrogen adsorption (continuous) and desorption (dashed) isotherms of MSU-2 silica in function of the pH of the initial surfactant solution of Triton X 100. As the pH increases, the adsorption jump moves toward higher relative pressure. The isotherms were shifted for visual facilitation.

and de Boer (BdB) method calculated on the desorption branch.^{13,34,35} The X-ray diffraction patterns were recorded with a Bruker D5000 diffractometer in Bragg–Brentano reflection geometry. Cu- $L_{3,2}$ radiation was employed that was monochromatized by a graphite single crystal in the diffracted beam. These X-ray patterns exhibit a single peak that was fitted by a Gaussian curve, after background subtraction, to determine both the d spacing and the peak broadening (fwhm).

2.2. Synthesis. The general synthesis procedure is based on the addition of the silicon alkoxide (TEOS) to a diluted solution of nonionic surfactant (0.02 M) with a TEOS/surfactant molar ratio of 6–10. After a rest time, a solution of sodium fluoride (NaF/TEOS = 0 to 4 mol %) is added to induce the silica condensation. The mixture is then kept for 36 h in a thermostated shaking bath, and the powder so-obtained is filtered, dried, and calcined in air at 200 °C for 6 h and then at 620 °C for 6 h.

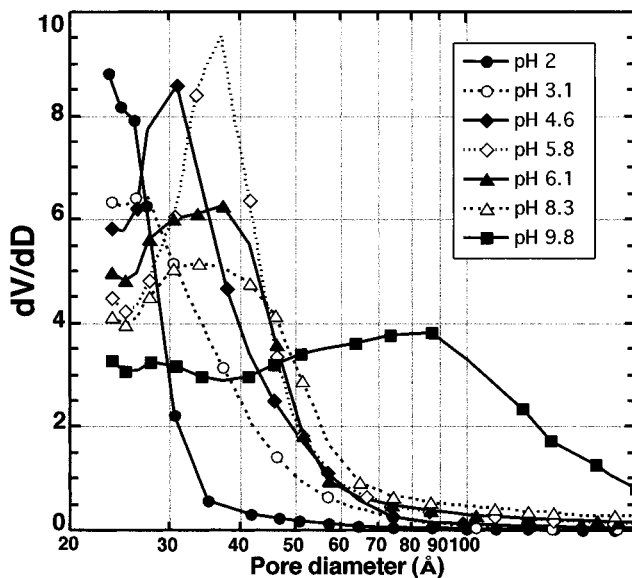


Figure 3. Broekhoff and de Boer pore size distribution deduced from the nitrogen desorption isotherm of MSU-2 silica as a function of the pH of the initial surfactant solution. From pH 1 to pH 5.8, the mean pore size increases from 2.5 to ~4.0 nm. After pH 5.8, this porous framework is less and less structured until pH 9.8 where it is characteristic of an amorphous silica gel.

We undertook to study the influence of pH on the material synthesized according to the procedure described above. In a first series of syntheses, the pH of the surfactant solution was adjusted between 1 and 10 prior to the addition of TEOS. This was done by either the addition of HCl (1.6 N) or NaOH (N) to a 0.02 M solution of Triton X 100. The remaining of the synthesis was the same: the TEOS/surfactant molar ratio was set to 8 (TEOS was added under both mechanical and ultrasonic stirring) and NaF was then added with a molar ratio NaF/TEOS = 2%. The mixture was kept under shaking for 12 h, at 35 °C. Syntheses were performed with solutions at pH adjusted between 0 and 9.8. Tests above pH 9.8 did not produce any solid.

The second set of syntheses involved a pH adjustment at pH 2, which can be performed either before or after the TEOS addition. In a typical synthesis, 3.33 g of TEOS (molar ratio TEOS/surf. = 8) was dispersed using a 2-min ultrasonic or mechanical stirring to 100 cm³ of a 0.02 M solution of surfactant (1.48 g of Tergitol 15S12). When pH was adjusted before the TEOS addition, the solution remained transparent upon the addition of TEOS. When pH was adjusted after the TEOS addition, a milky emulsion was first observed as previously reported³⁶ but the addition of 1 mL of hydrochloric acid (0.25 M) (final pH ≈ 2.0) quickly broke this emulsion and the expected colorless solution containing both surfactant and silica precursor was obtained within 15 min. This second approach was shown to allow a broader pH adjustment since pH 4 instead of 2 led to the same results within about 1 h. This solution remained stable for days (a small amount of silica appeared only after 2 weeks). From this pristine solution, the pH could be adjusted by further addition of NaOH or HCl. However, unlike our previously reported syntheses where TEOS and surfactants were first mixed in neutral pH (~6) without any reaction,^{13,14} returning to a neutral pH with this new strategy quickly induced the precipitation of a poorly

(34) Broekhoff, J. C. P.; de Boer, J. H. *J. Catal.* **1968**, *10*, 377.

(35) Galarneau, A.; Desplandier, D.; Dutartre, R.; Di Renzo, F. *Mesoporous Mater.* **1999**, *27*, 297.

(36) Cot, F.; Kooyman, P. J.; Larbot, A.; Prouzet, E. In *Mesoporous Molecular Sieves 1998*; Bonneviot, L., Beland, F., Danumah, C., Giasson, S., Kaliaguine, S., Eds.; Elsevier Science: Amsterdam, 1998; Vol. 117, p 231.

ordered silica. At pH 2, the solution was left at rest for 18 h and the condensation of silica was achieved by the addition of 0.65 mL of a 0.238 M solution of sodium fluoride (NaF/TEOS = 1 mol %). Reaction started after about 1 h and although it was almost totally achieved after 6 h, the mixture was kept at 35 °C for 3 days, in a thermostated shaking bath. The white powder so-obtained was filtered, dried, and calcined in air at 620 °C for 6 h after a 6 h step at 200 °C (3 °C min⁻¹ rate). Because of their heavy molecular weight, syntheses implying block-copolymers were based on weight ratios. For example, the synthesis using Pluronic P123 used a solution of 1.5 g of surfactant dissolved in 100 cm³ of water, kept at 40 °C; and the further addition of 3.3 g of TEOS.

When TMB was added as a swelling agent, the initial mixing was slightly different. For a TMB, surfactant molar ratio of 1, 0.240 g of TMB was first mixed with 1.476 g of Tergitol 15-S-12 and kept under stirring for 30 min in a capped vessel. This solution was added to 96 mL of water, and TEOS was then added to this mixture and kept under stirring for 30 min, with the final pH adjusted at 2 by the addition of 4 mL of HCl (0.25 N).

Syntheses using Tween 40 or 60 as templating agents, leading to MSU-4¹³ were also carried out in a different way because these surfactants are slightly soluble in water. To this purpose, TEOS was first added to the pure solution of surfactant, which was homogenized by stirring for 30 min (at 45 °C for the Tween 60) in a capped vessel. This solution was added dropwise to water and the remainder of the process was the same as described for the general pathway.

3. Results

3.1. Syntheses with a Wide pH Range. SEM pictures of calcined samples prepared at different pH with Triton X 100 are displayed in Figure 1. Between pH 1 and 2, a mixture of micrometric (~3 μm) sized particles that exhibit different shapes is observed: spheres (A), gyroids (B), and short hexagonal-shaped fibers (C and C'). These shapes were first identified in the growth of MCM-41 mesoporous silica particles using long chain ammonium compounds instead of nonionic PEO, which were synthesized in mild acidic conditions.³⁷ It was established that addition of ethanol at a pH below 1 favored the transformation of fibers to gyroids and then to spheres.^{37–39} When the pH increases up to pH 3, there is a progressive loss of defined shape of the particles that lose progressively their pristine shape, accompanied by a particle size decreasing below the micrometer, up to pH 8, where 200-nm ill-defined particles are obtained. At pH close to 10, the particles have evolved toward a nanometric size. This morphology change goes along with a change of the *d* spacing. As previously reported, X-ray patterns exhibit a single peak that we assigned to the pore-to-pore center correlation distance in these 3D worm-hole like structures, which we will refer to as the *d* spacing in the following.¹⁴ Both the *d* spacing and peak broadening (characterized by the full width at half maximum (fwhm) of the fitted Gaussian peak) evolutions with pH are given in Table 1. One observes constant values for both the *d* spacing (~3.7 nm) and the peak broadening (fwhm ≈ 1.5 nm)

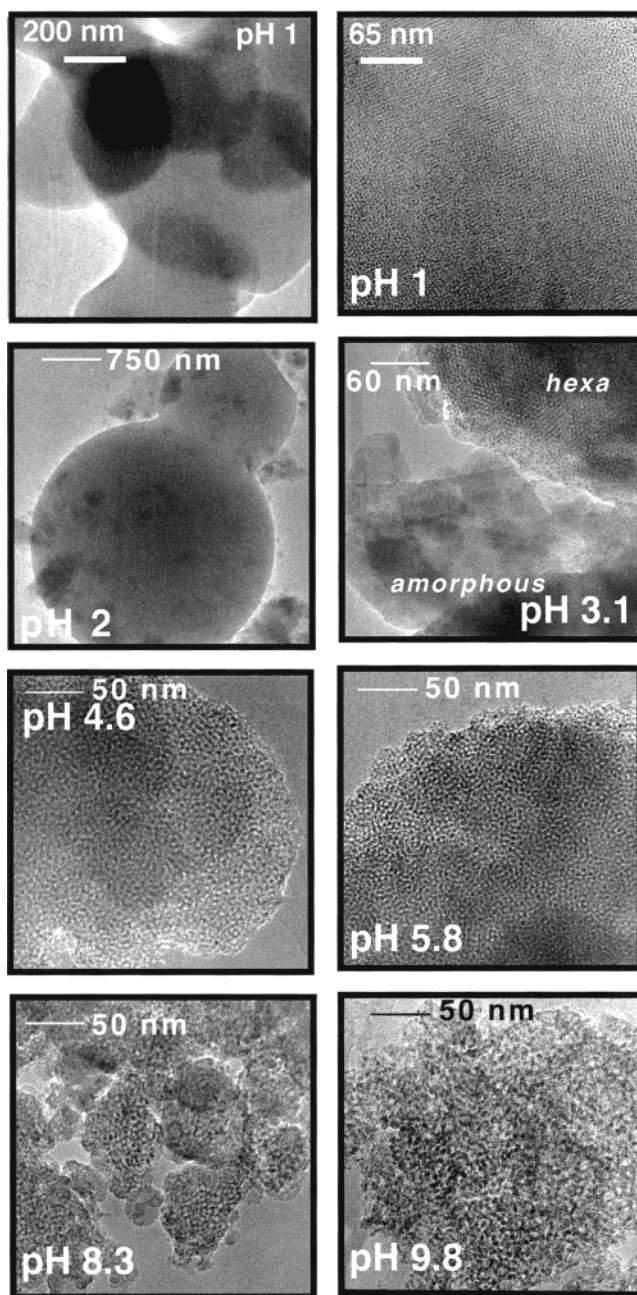


Figure 4. TEM observations of calcined MSU-2 silica synthesized with aqueous solutions of Triton X 100 preliminarily adjusted at different pHs. As the pH increases, the nanostructure evolves from a well-defined microporosity (pH 1 and 2) to 3D mesopores (pH 4.6 and 5.8) before a progressive amorphization of this material (pH 9.8). Samples synthesized at intermediary pH contain mixed structures: at pH 3.1, both amorphous and hexagonal symmetry structures exist and at pH 8.3, some small porous particles are still included in an amorphous matrix.

at pH between 0 and 2. For less acidic solutions, there is a continuous increase of the correlation distance, from pH 2 to 6, which goes from 4.4 nm up to 5.2 nm, along with broader peaks (fwhm ≥ 2.3 nm). The synthesis performed at pH 9 gave an amorphous X-ray pattern. A similar trend is observed on the nitrogen adsorption/desorption isotherms (Figure 2). The pH 0 to 2 isotherms are characteristic of microporous (≤1.5 nm) to supermicroporous (≤2.0 nm) structures. For pH 3.1 and 4.6, the isotherms reveal mixtures of structures observed at

(37) Yang, H.; Vovk, G.; Coombs, N.; Sokolov, I.; Ozin, G. A. *J. Mater. Chem.* **1998**, *8*, 743.

(38) Ozin, G. A.; Kresge, C. T.; Yang, H. In *Mesoporous Molecular Sieves 1998*; Bonnevot, L.; Beland, F.; Danumah, C.; Giasson, S.; Kaliaguine, S., Eds.; Elsevier Science: Amsterdam, 1998; Vol. 117, p 119.

(39) Di Renzo, F.; Testa, F.; Chen, J. D.; Cambon, H.; Galarneau, A.; Plee, D.; Fajula, F. *Microporous Mesoporous Mater.* **1999**, *28*, 437.

Table 2. Physicochemical Properties of MSU-1 Silica Synthesized with Linear Nonionic Surfactants of the Tergitol family (T 15SN:(CH₃)(CH₂)₁₄(EO)_N)

surfactant	TEOS/surf. ^a	NaF ^b (%)	pH	<i>d</i> spacing (nm)	pore size ^c (nm)	wall thickness ^d (nm)	surface area (m ² g ⁻¹)	V _p ^e (cm ³ g ⁻¹)	yield (%)
T 15S9	4	2	2.0	4.0	2.8	1.2	976	0.51	83
T 15S9	8	0	4.9 ^f	3.9	2.8	1.1	825	0.42	100
T 15S9	8	0	5.6 ^f	4.0	3.1	0.9	744	0.45	
T 15S9	8	1	2.0	4.2	2.8	1.4	910	0.48	95
T 15S9	8	4	2.0	4.5	3.6	0.9	1062	0.83	96
T 15S9	8	6	2.0	4.5	3.7	0.8	1028	0.86	94
T 15S9	10	2	2.0	4.2	3.1	1.1	968	0.58	94
T 15S9	12	2	2.0	4.3	3.3	1.0	869	0.75	95
T 15S12	8	0	4.9 ^f	4.0	2.7	1.3	712	0.34	100
T 15S12	8	0.5	2.0	3.8	2.3 (BJH)	1.5	723	0.34	89
T 15S12	8	1	2.0	4.0	2.4 (BJH)	1.6	910	0.44	94
T 15S12	8	2	2.0	4.2	3.0	1.2	1078	0.60	93
T 15S12	8	4	2.0	4.7	3.5	1.2	1053	0.76	98
T 15S12	8	6	2.0	5.2	3.7	1.4	1008	0.79	95
T 15S15	4	2	2.0	4.2	2.5	1.7	848	0.40	90
T 15S15	6	2	2.0	4.3	2.7	1.6	931	0.45	95
T 15S15	8	0	2.0	4.3	3.0	1.3	650	0.50	—
T 15S15	8	0	4.7 ^f	4.1	2.4 (BJH)	1.7	590	0.27	100
T 15S15	8	0.5	2.0	3.9	2.5	1.4	702	0.33	88
T 15S15	8	2	2.0	4.4	2.8	1.5	1000	0.52	93
T 15S15	8	4	2.0	4.7	3.4	1.3	1013	0.67	96
T 15S15	8	6	2.0	4.9	3.7	1.1	1027	0.77	95
T 15S15	12	2	2.0	4.4	2.9	1.5	989	0.53	98

^a Molar ratio. ^b NaF/TEOS molar ratio. ^c The pore size distribution was determined by the Broekhoff and de Boer method or by the Barret-Joyner-Hallenda one when indicated. ^d Because of the disordered porous framework, wall thickness was calculated by subtracting the pore diameter from the *d* spacing. ^e V_p, the total porous volume, was determined as the total adsorbed volume for *P/P*₀ ≈ 0.99. ^f The solutions were first homogeneized at pH 2, left at rest overnight, and the pH was adjusted by KOH addition.

Table 3. Physicochemical Properties of MSU-4 Silica Synthesized with Ethoxylated Sorbitan Surfactants

surfactant	TEOS/surf. ^a	NaF ^b (%)	pH	<i>d</i> spacing (nm)	pore size ^c (nm)	wall thickness ^d (nm)	surface area (m ² g ⁻¹)	V _p ^e (cm ³ g ⁻¹)	yield (%)
Tween 20	8	0	4.7 ^f	4.2	2.7	1.5	603	0.29	100
Tween 20	8	1	2.0	4.4	2.6	1.7	779	0.38	90
Tween 20	8	4	2.0	4.8	3.5	1.3	1087	0.76	
Tween 40	8	0	5.0 ^f	4.8	3.5	1.2	680	0.53	93
Tween 40	8	1	2.0	4.5	3.0	1.5	765	0.41	94
Tween 40	8	4	2.0	4.9	3.9	1.0	868	0.65	
Tween 60	8	0	2.0	4.4	2.9	1.5	662	0.34	
Tween 60	8	0	5.2 ^f	5.1	3.7	1.3	504	0.60	97
Tween 60	8	4	2.0	5.5	4.6	0.8	818	0.86	93
Tween 80	8	0	2.0	4.4	2.6	1.8	705	0.37	78
Tween 80	8	0	5.9 ^f	5.2	4.6	0.6	490	0.86	94
Tween 80	8	4	2.0	5.1	4.3	0.8	896	0.73	93
Pluronic F108	(2.2) ^g	2	2.0	11.6	4.6		694	0.46	46

^a Molar ratio. ^b NaF/TEOS molar ratio. ^c The pore size distribution was determined by the Broekhoff and de Boer method. ^d Because of the disordered porous framework, wall thickness was calculated by subtracting the pore diameter from the *d* spacing; ^e V_p, the total porous volume, was determined as the total adsorbed volume for *P/P*₀ ≈ 0.99. ^f The solutions were first homogeneized at pH 2, left at rest overnight, and the pH was adjusted by KOH addition. ^g Due to the heavy molecular weight of Pluronic F 108, the synthesis was performed on the basis of weight ratio with 3.3 g of TEOS for 1.5 g of copolymer.

pH 2 and pH 5.8 (neutral deionized water in our case). This latter synthesis, which is similar to previously reported syntheses,¹⁴ exhibits again a quite well reversible isotherm, with an increase of the adsorption jump toward higher relative pressures up to *P/P*₀ ≈ 0.4, that is a jump characteristic of small mesoporosity.⁴⁰ As the pH increases, a second adsorption step at *P/P*₀ > 0.9, which is characteristic of textural interparticle macroporosity, appears, and the mesoporous related step vanishes. Finally, the sample synthesized with an initial solution adjusted to pH 9.8 exhibits a nitrogen isotherm characteristic of an amorphous silica gel. This latter isotherm can be compared to SEM observations that only showed small particles. This allowed us to assign the broad adsorption jump for the sample prepared at pH 9.8 to the interparticle porosity between these particles. The pore diameter distributions calculated with the BdB model are displayed in Figure 3 and in

Table 1. Pore distributions below pH 2 could not be plotted since the BdB method only applies to mesoporous pores where there is a condensation process. Between pH 2 and pH 5.8, there is a continuous pore size increase from 2.5 nm up to ~4.0 nm. Above pH 5.8, the mean pore size remains constant up to pH 8.3, along with a broadening of the distribution. Finally, at pH 9.8, the pore distribution is very broad, characteristic of an amorphous mesoporous silica gel. Similarly, TEM clearly shows that the initial surfactant solution pH has a strong influence on the microstructure of the final material (Figure 4). Samples synthesized with an acidic pH consist of well defined particles, with a small porosity extended to the whole particle. This porosity can give well-ordered areas as shown in the Figure 4

(40) Gregg, S. J.; Sing, K. S. W. *Adsorption, Surface Area, and Porosity*, Academic: London 1983.

(pH 1, right, top). As the pH increases up to 3, the nitrogen isotherm does not exhibit a narrow adsorption jump anymore. Indeed, TEM shows that the pH 3.1 sample consists partly of quite amorphous particles, partly of hexagonal MCM-41-like areas that have been reported elsewhere.²⁷ A rather neutral pH leads to the well-known worm-hole like structure (see pH 4.6 and 5.8 images in Figure 4), which is progressively destroyed upon increasing the pH. For pH 8.3, only small disordered porous particles remain and the synthesis at pH 9.8 yields only amorphous material.

3.2. Syntheses in a Mild Acid Medium. When TEOS is added under ultrasonic treatment to a neutral solution (actual pH was 5.8), a milky emulsion is obtained. If the sonication conditions are carefully adjusted, a phase demixing between a water-rich microemulsion and an organic-rich foam occurs after several hours of rest. In previous syntheses; this foam was removed before the addition of fluoride. We demonstrated that changing the sonication conditions, allowed us to synthesize either dense nanometric particles¹⁴ or empty hollow spheres.^{36, 41}

If a small amount of acid is added to this milky emulsion, the emulsion is quickly broken (within 10 min at pH 2, or 4 h at pH 4), and a homogeneous colorless solution is then obtained. This aqueous solution consists of isolated micellar hybrid objects of 6–10 nm diameter, depending on the TEOS/surfactant ratio (dynamic light scattering results not shown in this report). It is rather stable with time since no significant silica condensation is observed if one does not add fluoride. However, a significant reaction yield is obtained if one raises the pH up to ~6.0. This stability allowed us to let the solutions for rest for almost 12 h before adding the catalyst or increasing the pH. All syntheses were aged at 35 °C under a slow shaking for 3 days but reaction had already been completed after 12 h. These syntheses were performed with different types of surfactants or block copolymers, various TEOS/surfactant ratios and amounts of fluoride (see Tables 2 and 3).

From the stable solution prepared at pH 2, there are two ways to induce the silica condensation. Therefore, we compared the X-ray patterns and nitrogen isotherms of MSU-1 silica, synthesized with Tergitol 15-S-12 at pH 2, with a NaF/TEOS molar ratio of 4%, with that synthesized without fluoride but with a pH increase from 2 to 6. On the X-ray patterns, displayed in Figure 5, one sees that the material obtained by the pH increase is much less structured than the material prepared by a fluoride catalysis. This is confirmed by the different isotherms plotted in Figure 6. Using fluoride instead of pH leads also to different particle sizes. SEM (Figure 7) shows that the synthesis with fluoride allowed us to obtain rather monodisperse particles in the micrometric range (Figure 7a), which explains why they do not exhibit any textural porosity. Actually, an accurate adjustment of the synthesis parameters allowed us to prepare powders of monodisperse spherical particles in the 5 μm range, suitable for chromatography applications.^{29,30} Unlike the fluoride-helped synthesis, the synthesis without fluoride leads

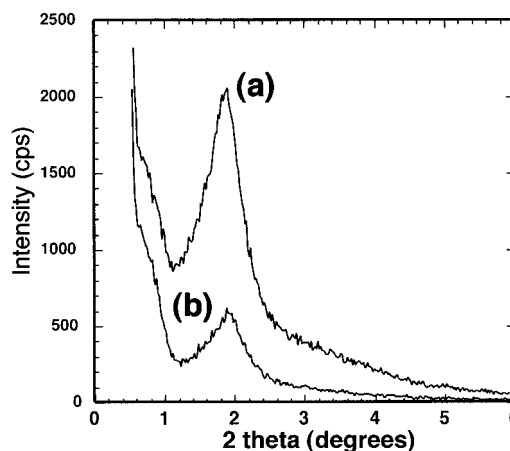


Figure 5. X-ray pattern of calcined MSU-1 silica synthesized through the double-step reaction with Tergitol 15-S-12. After a preliminary structuration step at pH 2, the silica condensation was induced by (a) the addition of a NaF/TEOS molar ratio of 4% and (b) a pH increase up to pH 6. These patterns exhibit a single correlation peak due to the 3D worm-hole like porous framework.

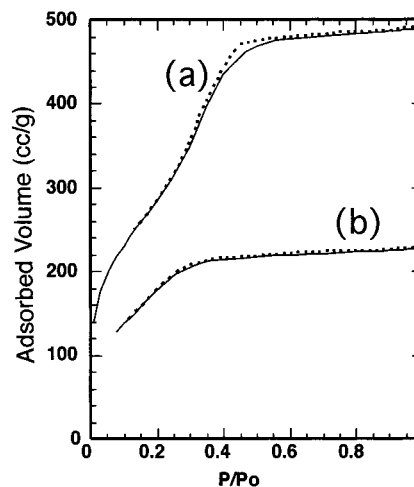


Figure 6. Evolution of the nitrogen adsorption (continuous) and desorption (dashed) isotherms synthesized through the double-step reaction with Tergitol 15-S-12, after a preliminary structuration step at pH 2 and a silica condensation induced by (a) the addition of a NaF/TEOS molar ratio of 4% and (b) a pH increase up to pH 6

to a broader distribution, mainly in the submicrometer range (Figure 7b).

This synthesis implying a first assembly step at pH ≈ 2 –4, followed by a fluoride-helped condensation step, allowed us to add a swelling agent such as TMB. The addition of TMB gave also a well-structured material. The nitrogen isotherms shows that a TMB:surfactant molar ratio of 1 leads to a mean pore size shift from 3 to 4.5 nm (Figure 8). Finally the TEM observation confirmed that all materials of the MSU-1 family exhibited the expected 3D worm-hole porous framework (Figure 9).¹⁰

We observed also that the synthesis using Tween-60 or Pluronic P 123 copolymer as template agents led to very well ordered material that exhibited X-ray patterns (Figure 10) and the corresponding nitrogen adsorption/desorption isotherm (Figure 11) characteristic of a MCM-41-like hexagonal framework, with mean pore

(41) Kooyman, P. J.; Verhoef, M. J.; Prouzet, E. In *Nanoporous Materials II*; Sayari, A., Jaroniec, M., Pinnavaia, T. J., Eds.; Elsevier Science BV.: Banff, Alberta, Canada, 2000; Vol. 129, pp 535.

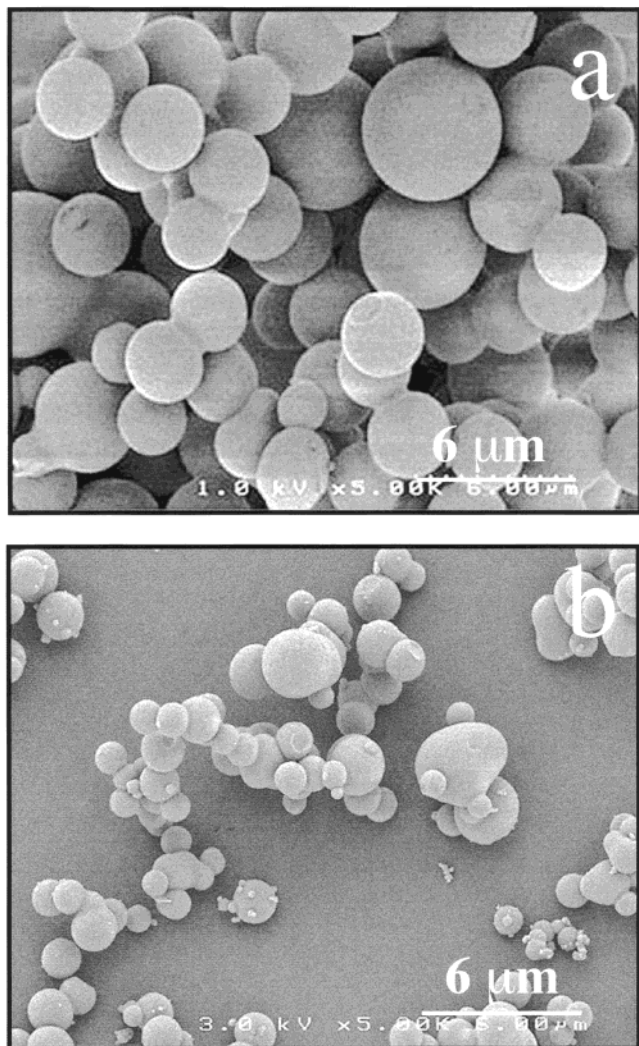


Figure 7. SEM observation of calcined MSU-1 silica synthesized through the double-step reaction with Tergitol 15-S-12, after a preliminary structuration step at pH 2 and a silica condensation induced by (a) the addition of a NaF/TEOS molar ratio of 4% and (b) a pH increase up to pH 6. (Scale is 6 μm .)

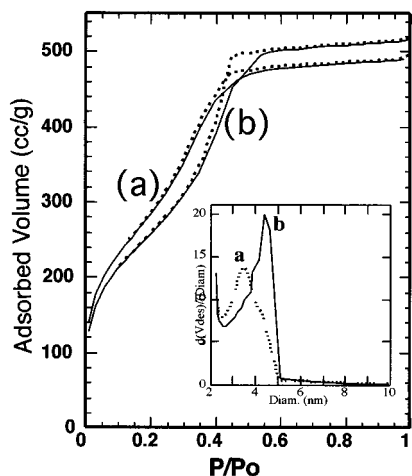


Figure 8. Evolution of the nitrogen adsorption (continuous) and desorption (dashed) isotherms for MSU-1 silica (a) without the addition of TMB and (b) with a TMB/Tergitol 15-S-12 molar ratio of 1. Inset: BdB pore size distribution. The addition of TMB enlarges the pore from 3.5 to 4.5 nm.

diameters equal to 4.5 and 8.2 nm for Tween 60 and Pluronic P 123, respectively.¹ SEM shows that all

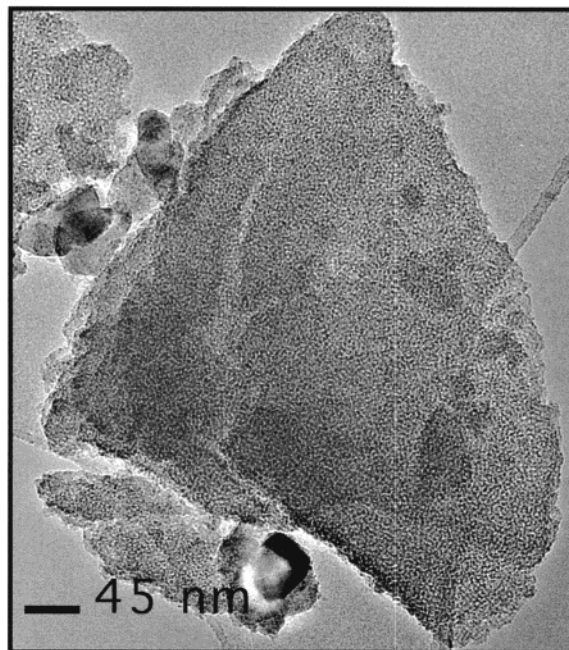


Figure 9. TEM observation of calcined MSU-1 silica synthesized with Tergitol 15-S-12 and a NaF/TEOS molar ratio of 2%.

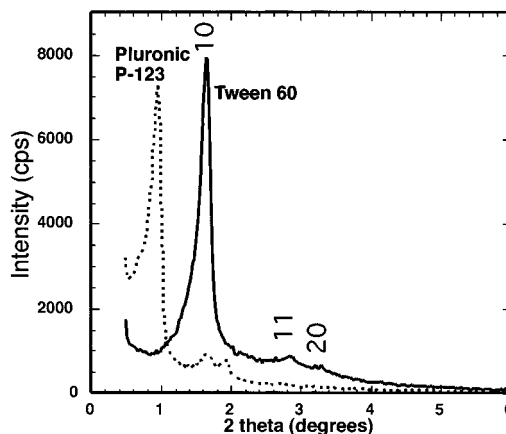


Figure 10. X-ray pattern of a calcined MSU-4 silica synthesized with Tween 60 (line) and Pluronic P 123 (dashed). These X-ray patterns exhibit well-defined peaks characteristic of a hexagonal symmetry.

particles exhibit a similar geometry with particles edges close to 120° (see Figure 12), but MSU silica synthesized with Tween 60 or Pluronic P 123 exhibit different particle morphologies: MSU-4 synthesized with Tween 60 exhibits a morphology similar to that observed with MCM-41 particles,¹ whereas MSU-3 prepared with the copolymer is mainly composed of $1.5 \times 0.3 \mu\text{m}$ rodlike particles (some spherical particles were observed, too). Such particles were obtained with sodium metasilicate and cationic surfactants⁴² and a similar synthesis, performed with Pluronic P 123, fluoride, in more acidic medium led also to longer fibers of a mesoporous SBA-15-type material.⁴³ TEM confirms this hexagonal symmetry (Figure 13). Rodlike particles prepared with Pluronic P 123 are particularly well-ordered since the

(42) Shio, S.; Kimura, A.; Yamaguchi, M.; Yoshida, K.; Kuroda, K. *J. Chem. Soc., Chem. Commun.* **1998**, 2461.

(43) Schmidt-Winkel, P.; Yang, P.; Margolese, D. I.; Chmelka, B. F.; Stucky, G. D. *Adv. Mater.* **1999**, *11*, 303.

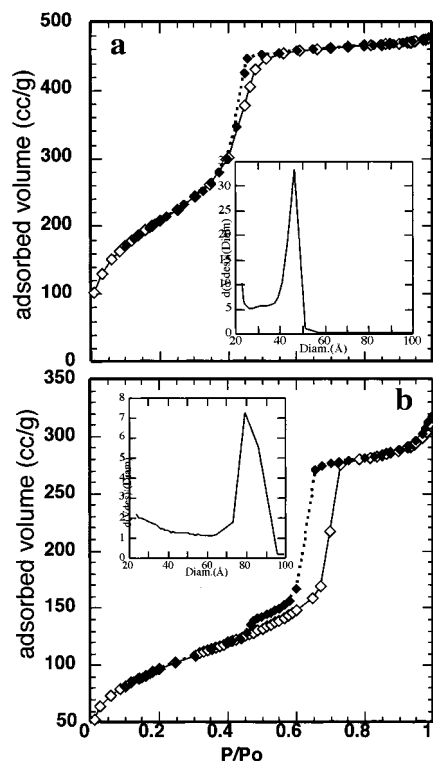


Figure 11. Nitrogen adsorption (\diamond) and desorption (\blacklozenge) isotherms of the calcined MSU-4 silica synthesized at 45 °C, with Tween 60 (up) and Pluronic P-123 (down). Inset: BdB pore size distribution.

pores are aligned along the main axis and perfectly hexagonally stacked as can be seen on the section.

4. Discussion

The first attempts to use nonionic PEO-based surfactants for the synthesis of MTS led to the so-called MSU-X family.¹⁰ Two main synthesis pathways for MSU-X using neutral pH conditions and more or less diluted solutions have been defined,^{10,14} whereas other approaches using either a direct synthesis or electrochemical-assisted synthesis of an inorganic framework in a lyotropic liquid crystal or syntheses in highly acidic block-copolymers aqueous solutions,^{15–17,19} have also been very successful. Historically, the first pathway for the synthesis of MSU-X materials (Pathway I) was a 16 h synthesis at room temperature under strong mechanical stirring of a ~ 0.2 M solution of surfactant with a TEOS/surfactant molar ratio of 8.¹⁰ This pathway was recently reexplored by Bagshaw et al. through an acidic ($N^0(N^+)X^-I^+$ route) or basic ($N^0M^+I^-$ route) synthesis.⁴⁴ They obtained materials that exhibited quite broad diffraction peaks but in parallel, a hydrothermal postsynthesis treatment applied to materials synthesized along pathway I, gave materials (named SAB) with well-defined hexagonal porous structure similar to that observed in MCM-41 materials.²⁰ A second pathway (pathway II) involved a more dilute solution (0.02 M solution of surfactant, molar TEOS/surfactant = 8) with first a dispersion of TEOS by ultrasonic treatment followed by a resting time to allow one to remove an organic-rich supernatant emulsion.

(44) Bagshaw, S. A.; Kemmitt, T.; Milestone, N. B. *Microporous Mesoporous Mater.* **1998**, *22*, 419.

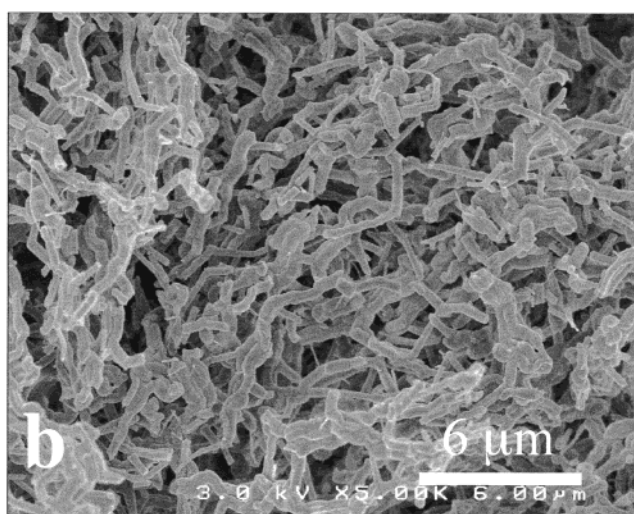
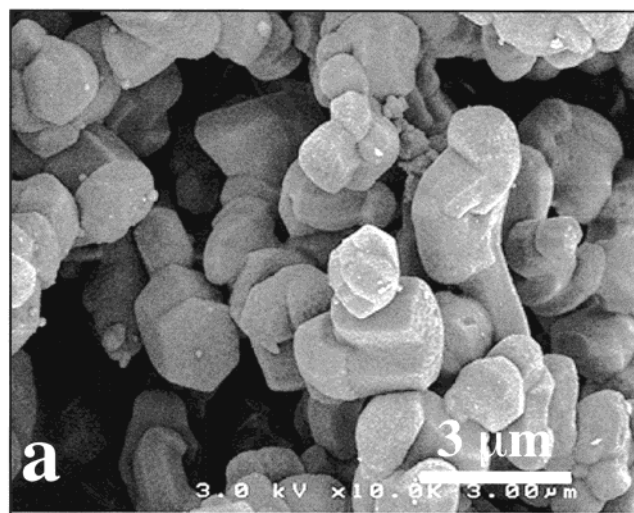


Figure 12. SEM observation of the calcined MSU-4 silica synthesized at 45 °C, with (a) Tween 60 and (b) Pluronic P-123. Although the synthesis conditions are rather similar, the nature of the surfactant has a strong effect on the morphology of particles.

This synthesis implied the addition of sodium fluoride to the remaining colorless solution in order to catalyze the silica condensation.¹⁴ Fluoride ion has been used in the synthesis of different mesoporous molecular sieves.^{43,45,46} Stucky et al.^{47,48} were the first to point out that the synthesis of micelle templated structures (MTS) is based on specific interactions between organic molecules and inorganic species that lead to a hybrid organic/inorganic mesophase prior to the reaction. Since then, Galarneau et al. showed that during the synthesis of MCM-41, an initial amorphous gel made from cationic surfactants (CTAB) and inorganic species, was quickly restructured to lead to the hexagonal shaped material.⁴⁹

(45) Silva, F. H. P.; Pastore, H. O. *J. Chem. Soc., Chem. Commun.* **1996**, 833.

(46) Voegtlin, A. C.; Ruch, F.; Guth, J. L.; Patarin, J.; Huve, L. *Microporous Mater.* **1997**, *9*, 97.

(47) Monnier, A.; Schüth, F.; Huo, Q.; Kumar, D.; Margolese, D. I.; Maxwell, R. S.; Stucky, G. D.; Krishnamurty, M.; Petroff, P. M.; Firouzi, A., et al. *Science* **1993**, *261*, 1299.

(48) Huo, Q.; Margolese, D. I.; Ciesla, U.; Feng, P.; Gier, T. E.; Sieger, P.; Leon, R.; Petroff, P. M.; Schüth, F.; Stucky, G. D. *Nature* **1994**, *368*, 317.

(49) Galarneau, A.; Di Renzo, F.; Fajula, F.; Mollo, L.; Fubini, B.; Ottaviani, M. F. *J. Colloid Interface Sci.* **1998**, *201*, 105.

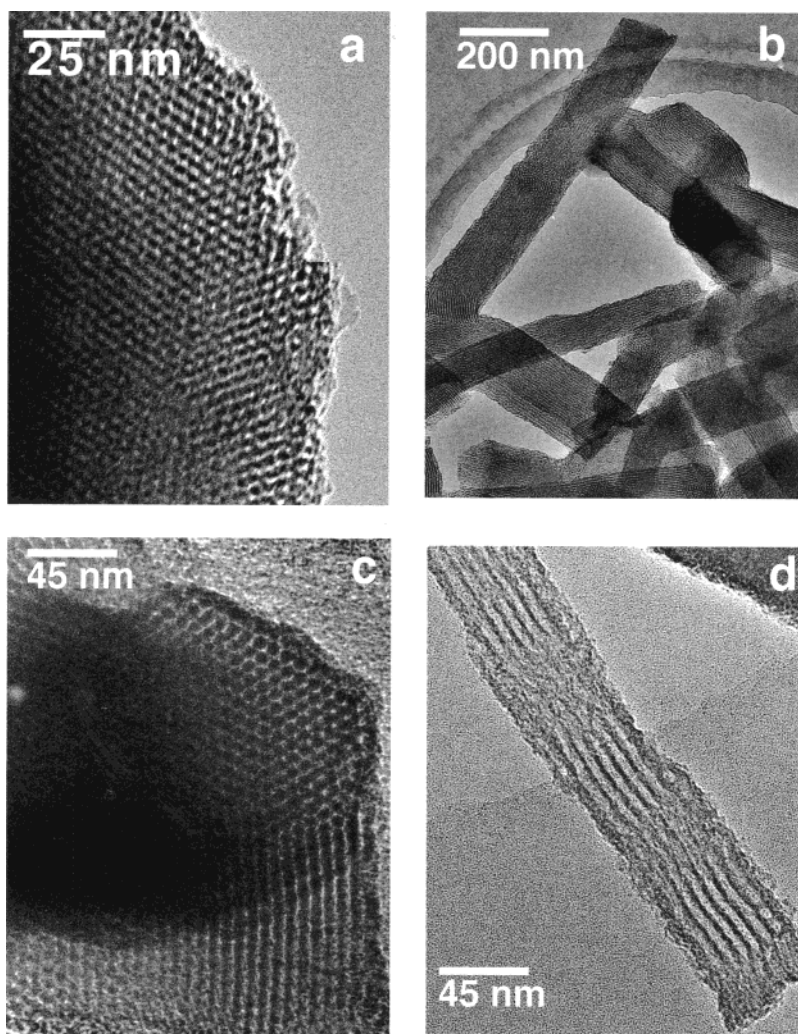


Figure 13. TEM observation of the calcined MSU-4 silica synthesized at 45 °C, with Tween 60 (photo a) and Pluronic P 123 (photos b to d). Hexagonal-shaped particles obtained with Tween 60 exhibit a hexagonal pore framework similar to that of MCM-41. Rodlike particles obtained with Pluronic P 123 are made of long pores parallel to the main axis (photo b) and hexagonally stacked (photo c). Some particles exhibit a fiber shape with a thickness of 50 nm and a micrometric length (photo d).

However the electrically neutral $N^{0}I^0$ assembly mechanism between TEOS and the ethylene oxide groups of a nonionic PEO surfactant occurs through hydrogen bonds that are much weaker than electrostatic interactions. Thus, both the final nanostructure and morphology of the MSU-X are highly dependent on the initial preparation procedure that will settle the final order between TEOS molecules and PEO surfactants. Therefore, parameters such as the local interactions created by the lipophile/hydrophile balance, which is temperature dependent, the Brownian motion that destroys the framework (that is also temperature dependent), the presence of different ions in the close neighborhood^{27,28} as well as the relative hydrolysis and polymerization kinetics will modify the organization of this highly dynamic hybrid system. Besides, this synthesis occurs with dilute conditions where the hybrid objects form an isotropic aqueous phase instead of a gel. With regard to this whole set of parameters, it appears that reproducible conditions are obtained only if one manages to prepare a stable and homogeneous solution before inducing the condensation process.

Compared with the previous ways of preparation of MSU-X silica, namely the pathways I and II, the new

process described in this paper, which we call pathway III, provides a new insight of the synthesis of MSU-X silica because it proceeds from a double-step mechanism that separates the assembly step from the condensation step. The distinguishing feature of the new pathway III compared to pathways I and II is thus the possibility to accurately tune the initial assembly step. In the first part of this report, adjusting the pH in a wide range prior to the addition of TEOS gave totally different materials because both the homogenization step (that is the structure-determining step) and the condensation step were mixed if the pH is either too low or too high. It appeared that the mild acidity range ($1 < \text{pH} < 4$) allows the formation of micellar hybrid objects built with surfactants and silica oligomers (the TEOS hydrolysis rate is high at pH 2–4), with a quite narrow size distribution (6–10 nm objects, depending on the TEOS/surfactant ratio). As long as the pH is maintained in the 2–4 range, these objects remain stable because the silica condensation rate is very low.⁵⁰ At this stage, they can be destabilized by either a pH increase or the addition of a catalyst. Increasing the pH gives a meso-

(50) Brinker, C. J. *J. Non Cryst. Solids* **1988**, *100*, 31.

porous material but the condensation step is too fast to allow a good structuration. Hence one obtains materials with a poorly ordered porosity. Furthermore, since the reaction is induced all over the volume of the reactor, the competition between many nucleation/growth processes leads to small particles with a broad size distribution. The addition of fluoride instead of the pH increase is suitable because it creates a small amount of seeds whose concentration depends only on the fluoride amount. Thus, the further growth of particles, fed by the whole homogeneous medium, follows a more controllable isotropic growth process, which mostly leads to spherical particles with a total yield close to 100%. An accurate control of some synthesis parameters such as concentration or fluoride/TEOS ratio allowed us to obtain rather well monodispersed powders in the 5 μm size range.²⁹

The main proof of the different mechanism involved in this process is that it leads to different structures than those obtained with previous synthesis pathways. The best example is provided by MSU-4 silicas, using Tween surfactants as templating agents. When the synthesis is carried out according to pathway II, that is in neutral pH, one obtains powders made of nanometric sized particles with a double porosity, a structural one due to the organic surfactant framework and a textural one due to the interparticle porosity related to the small size of these particles.¹³ Unlike pathway II, synthesis according to pathway III leads to micrometric sized particles.

Finally, this homogeneous micellar solution, which is the starting medium of the reaction induced by the fluorine-helped seeding, allows some aggregation mechanisms to occur. This is observed with Tween 60 and Pluronic P123 block-copolymer, which are less hydrophilic molecules than linear ones such as Tergitol 15-S-12. The association of the micellar hybrid objects, under specific reaction conditions, allows the system to find an energetically favorable conformation, with a hexagonal pore framework similar to that of MCM-41.⁵¹ Bagshaw showed that a hydrothermal postsynthesis treatment could also help the system to reach this stable structure.²⁰ It is the first time that such a structure is reported in mild acidity with a Tween molecules but a similar structure was reported by Schmidt-Winkel, Stucky et al. for Pluronic P123. They reported that fibers with well-ordered channels parallel to the main axis could be obtained over micrometer-length scales when the synthesis was conducted at $\text{pH} \leq 1.2$ (HCl:Si ratios of 6.0 or 0.6), with small amounts of fluoride. Increasing the pH above 1.2 gave bundles of highly bent and curved fibers. They assigned this specific morphology to the use of fluoride. We show in this report that short straight fibers of hexagonally structured MSU-type silica can be obtained in the range of pH above 1.2. Unlike the interpretation provided by Schmidt-Winkel, we do not assign this special structure to the use of fluoride, because it has been shown that different kind of nanostructures and morphologies can be obtained when using fluoride.^{13,14,29,36} Actually, we think that the kinetics of association by "trial and error" processes of the hybrid objects to find the most stable assembling can proceed as long as the structure is not frozen by the silica condensation.

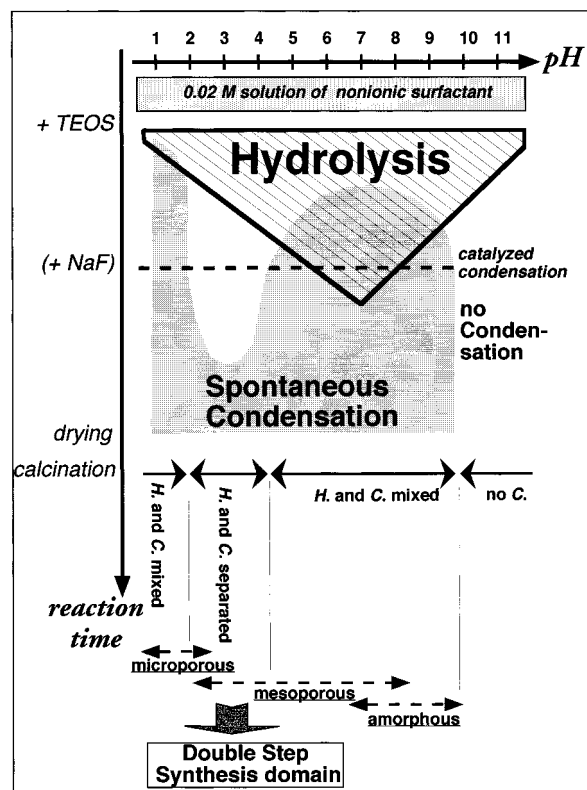


Figure 14. Picture of the different reaction mechanisms in function of the initial pH.

Finally, according to the general hydrolysis and condensation process drawn by Brinker,⁵⁰ the whole process can be summarized as displayed in Figure 14. It is important to specify that this scheme applies only for reactions in diluted media (namely [surf.] below 0.1 M). Both the kinetics of hydrolysis and condensation are strongly modified when the concentration increases, and it is obvious that this picture does not take into account the general synthesis conditions that were used for the preparation of SBA-15 type materials.¹⁵ The course of the reaction with time can be schematized in function of the initial pH. Thus, four domains can be identified in function of pH:

(i) For $\text{pH} \leq 2$, the hydrolysis time is short (the hydrolysis is fast) but the hydrolyzed species can stand a spontaneous condensation that will lead to the mixing of the assembly and condensation steps; an accurate control of the reaction is difficult because the addition of sodium fluoride will induce the polycondensation of a broader distribution of silicate oligomers.

(ii) Between approximately pH 2 and 4, the hydrolysis time is short and the condensation begins only after a long delay. This is a propitious situation to allow an easy separation of the hydrolysis and condensation steps. Hence, sodium fluoride can be added before the spontaneous condensation starts and it will catalyze the condensation of well-defined small silicate oligomers. The control of the reaction is much easier, and this opens the field of what we called the double-step synthesis.

(iii) Above pH 4 and up to pH 10, the same behavior as for acidic pH is observed.

(51) Yang, H.; Ozin, G. A.; Kresge, C. T. *Adv. Mater.* **1998**, *10*, 883.

(iv) Above pH 10, the silicates oligomers remain in solution and there is no way to precipitate any solid phase.

It must be also observed that the pH affects the material structure: microporous silica is obtained under acidic conditions whereas mesoporous, and then amorphous silica are synthesized as the medium becomes

more basic. Drawing the whole reaction pattern will require studying another parameter, that is the concentration. A full understanding of this versatile reaction behavior should be successful to unify the different synthesis processes that have been reported until now.

CM991188S